

Complete polarization control of light from a liquid crystal spatial light modulator

Ignacio Moreno,^{1,*} Jeffrey A. Davis,² Travis M Hernandez,² Don M. Cottrell,² and David Sand²

¹*Departamento de Ciencia de Materiales, Óptica y Tecnología Electrónica, Universidad Miguel Hernández, 03202 Elche, Spain*

²*Physics Department, San Diego State University, CA, USA*
i.moreno@umh.es

Abstract: We present a method to generate complete arbitrary spatially variant polarization modulation of a light beam by means of a parallel aligned nematic liquid crystal spatial light modulator (SLM). We first analyze the polarization modulation properties in a transmission mode. We encode diffraction gratings onto the SLM and show how to achieve partial polarization control of the zero order transmitted light. We then extend the technique to a double modulation scheme, which is implemented using a single SLM divided in two areas in a reflective configuration. The polarization states of the transmitted beam from the first pass through the first area are rotated using two passes through a quarter wave plate. The beam then passes through the second area of the SLM where additional polarization information can be encoded. By combining previously reported techniques, we can achieve complete amplitude, phase and polarization control for the diffracted light that allows the creation of arbitrary diffractive optical elements including polarization control. Theoretical analysis based on the Jones matrix formalism, as well as excellent experimental results are presented.

©2011 Optical Society of America

OCIS codes: (050.1970) Diffractive optics; (070.6120) Spatial light modulators; (230.5440) Polarization-selective devices.

References and links

1. J. E. Solomon, "Polarization imaging," *Appl. Opt.* **20**(9), 1537–1544 (1981).
2. J. A. Davis, G. H. Evans, and I. Moreno, "Polarization-multiplexed diffractive optical elements with liquid-crystal displays," *Appl. Opt.* **44**(19), 4049–4052 (2005).
3. Z. Bomzon, V. Kleiner, and E. Hasman, "Formation of radially and azimuthally polarized light using space-variant subwavelength metal stripe gratings," *Appl. Phys. Lett.* **79**(11), 1587–1589 (2001).
4. J. A. Davis, D. E. McNamara, D. M. Cottrell, and T. Sonehara, "Two-dimensional polarization encoding with a phase-only liquid-crystal spatial light modulator," *Appl. Opt.* **39**(10), 1549–1554 (2000).
5. X.-L. Wang, J. Ding, W.-J. Ni, C.-S. Guo, and H.-T. Wang, "Generation of arbitrary vector beams with a spatial light modulator and a common path interferometric arrangement," *Opt. Lett.* **32**(24), 3549–3551 (2007).
6. D. Preece, S. Keen, E. Botvinick, R. Bowman, M. Padgett, and J. Leach, "Independent polarisation control of multiple optical traps," *Opt. Express* **16**(20), 15897–15902 (2008).
7. C. Maurer, A. Jesacher, S. Fürhapter, S. Bernet, and M. Ritsch-Marte, "Tailoring of arbitrary optical vector beams," *New J. Phys.* **9**(3), 78 (2007).
8. J. A. Davis, D. M. Cottrell, J. Campos, M. J. Yzuel, and I. Moreno, "Encoding amplitude information onto phase-only filters," *Appl. Opt.* **38**(23), 5004–5013 (1999).
9. J. A. Davis, P. Tsai, D. M. Cottrell, T. Sonehara, and J. Amako, "Transmission variations in liquid crystal spatial light modulators caused by interference and diffraction effects," *Opt. Eng.* **38**(6), 1051–1057 (1999).
10. M. Taghi Tavassoly, I. Moaddel Haghighi, and K. Hassani, "Application of Fresnel diffraction from a phase step to the measurement of film thickness," *Appl. Opt.* **48**(29), 5497–5501 (2009).
11. J. A. Ferrari and J. L. Flores, "Nondirectional edge enhancement by contrast-reverted low-pass Fourier filtering," *Appl. Opt.* **49**(17), 3291–3296 (2010).
12. J. L. Horner and P. D. Gianino, "Phase-only matched filtering," *Appl. Opt.* **23**(6), 812–816 (1984).
13. J. L. Horner and J. R. Leger, "Pattern recognition with binary phase-only filters," *Appl. Opt.* **24**(5), 609–611 (1985).

14. J. A. Davis, S. W. Flowers, D. M. Cottrell, and R. A. Lilly, "Smoothing of the edge-enhanced impulse response from binary phase-only filters using random binary patterns," *Appl. Opt.* **28**(15), 2987–2988 (1989).
 15. C. Zhou and L. Liu, "Numerical study of Dammann array illuminators," *Appl. Opt.* **34**(26), 5961–5969 (1995).
 16. I. Moreno, J. A. Davis, D. M. Cottrell, N. Zhang, and X.-C. Yuan, "Encoding generalized phase functions on Dammann gratings," *Opt. Lett.* **35**(10), 1536–1538 (2010).
 17. J. A. Davis, I. Moreno, and P. Tsai, "Polarization eigenstates for twisted-nematic liquid-crystal displays," *Appl. Opt.* **37**(5), 937–945 (1998).
 18. J. Nicolás and J. A. Davis, "Programmable wave plates using a twisted nematic liquid crystal display," *Opt. Eng.* **41**(12), 3004–3005 (2002).
 19. J. Luis Martínez, I. Moreno, J. A. Davis, T. J. Hernandez, and K. P. McAuley, "Extended phase modulation depth in twisted nematic liquid crystal displays," *Appl. Opt.* **49**(30), 5929–5937 (2010).
-

1. Introduction

The generation of two dimensional polarization distributions and polarizing diffractive elements is interesting for many applications including polarization imaging [1], data encoding, and polarization multiplexing [2]. Different methods to generate light beams with spatially structured polarization have been theoretically proposed and experimentally probed, including sub-wavelength grating structures [3] and liquid crystal spatial light modulators (LC-SLM) [4]. The latter are interesting because they have the advantage of providing programmable elements.

One valuable application of LC-SLMs as diffractive optical elements is the polarization control of transmitted light. This has been extremely hard to achieve because nearly all devices act on a single polarization component. Recently, some other approaches for spatial polarization control have been reported that obtain different polarization states on different diffraction orders [5], or that use a split screen configuration on a SLM so different actuation can be performed onto two different polarization components. For instance, in Ref [2], a system was demonstrated to generate polarization selective computer generated holograms, by using two SLMs. One device displayed two phase-only holograms on different halves, while the other one was used to control the corresponding output polarization. More recently, in Ref [6], a parallel aligned reflective liquid crystal display was employed to display blazed gratings with different orientations in order to generate optical traps in a microscope. For that purpose, the screen of the display was again divided in two halves, and a half-wave plate had to be placed in the beam reflected in only one half of the screen. In this work it was also demonstrated how the addition of a phase bias in one half of the screen with respect to the other allows control of the polarization state of the generated traps. Note that in these two systems, a homogeneous linear polarization state parallel to the LC director was required. An alternative system, again using a reflective SLM, was proposed in Ref [7], to generate vectorial laser beams, which used a Wollaston prism to spatially separate two orthogonal linear polarization components of the incoming light beam, and direct them to the two halves of the display screen. A half-wave plate was again required before one half of the input screen in order to align the incoming polarization with the LC director of the display. After recombination, a spatial polarization control of the reflected beam was demonstrated. Note that this system employs the two polarization components of the incoming light, thus being more light efficient and less sensitive to polarization misalignments.

Here we show a new architecture for polarization control that combines all the features of the these previous systems, based on a single parallel aligned transmissive SLM (instead of a reflective SLM), where we illuminate the SLM with light having both horizontal and vertical polarization states. However we utilize both polarization states in each of the single and double modulation systems that are presented.

We begin by analyzing the polarization control that can be achieved with a single modulation scheme. The parallel-aligned LC-SLM only diffracts the vertically polarized component of input light (which is parallel to the LC director). The horizontal component of input light is unaffected by the LC-SLM. In a previous work, we have developed various methods for controlling the phase and magnitude of the vertically polarized light [8]. We can control the fraction of light that is diffracted by controlling the modulation depth M_A of the diffraction grating that is encoded onto the SLM. We can also add a phase bias φ_A to the

grating, which is applied to both the zero and first diffracted orders, and adds control over the polarization state of the zero-order diffracted order. If the incident light onto the SLM has two polarization states, we can alter the polarization state of the zero order diffracted light.

Then, we will show how further control may be gained for systems in which the light is modulated twice, either by passing twice through the SLM or passing through a second SLM. In our approach, the transmitted beams from the first pass are reflected and their polarization states are rotated by 90 degrees by passing twice through a quarter wave plate. Now, the vertical polarization states become horizontally polarized, and the horizontal polarization state becomes vertically polarized. On the return pass, the light passes through a second diffraction grating having a modulation depth M_B and phase bias ϕ_B . The orientation and period of this second diffraction grating can be the same or different from the first. The new horizontally polarized component is unaffected, while the new vertically polarized component is diffracted dependent upon the modulation depth of the grating on the second pass. Consequently we can obtain polarization control over the total zero order and also over the first-order diffracted light. Experimental results are shown for both single and double modulation configurations.

Our approach differs from the system in Ref [7], in that we illuminate each half of the SLM with both polarization states allowing greater control because we can add separate spatially dependent amplitude and phase shifts on both passes. Therefore the beams from both passes can be modulated to contribute to the final polarization pattern. In addition, we avoid the necessity for a wave-plate that only covers half of the SLM screen, as was required in [6,7].

The paper is organized with four sections. After this introduction, Section 2 reviews the theory and shows experimental results demonstrating how we can obtain spatially variant polarization distributions for the single modulation case. Section 3 then shows the theory and experimental results for the double modulation case. Our experimental results for the double modulation configuration include computer generated holograms and Dammann gratings with polarization sensitivity. In this section we include also other results where we borrow the phase bias idea from [6] and extend it to generalized computer generated holograms that create arbitrary complex (amplitude and phase) distributions with arbitrary states of polarization. Finally, Section 4 includes the conclusions of the work.

To understand this model, we will look at this in more detail combining Jones vectors and gratings. We first consider the single modulation.

2. Single modulation theory and experimental results

The single modulation configuration (denoted by the subscript A) is shown schematically in Fig. 1. A linear polarizer is placed in the optical system aligned at an angle θ . Consequently the vertically polarized component is proportional to $\cos(\theta)$, while the horizontal component will be proportional to $\sin(\theta)$. This beam is incident onto a parallel aligned LC-SLM.

The horizontally polarized component is not affected by the LC-SLM and passes through unchanged as shown in Fig. 1(b). We can alter the vertically polarized light in two ways as shown in Fig. 1(a). First we can encode a diffraction grating onto the SLM that controls the amount and direction of the diffracted light. The general diffraction grating is written as $t_A(x) = \exp(iM_A 2\pi x / d_A)$. Here d_A is the period of the grating and M_A controls the depth of the phase for the grating where $0 \leq M_A \leq 1$. We note that the orientation and period of the diffraction grating can be easily adjusted and can vary spatially.

The fraction of diffracted light can be controlled through the modulation depth M_A of the diffraction grating as shown in Fig. 2(a). The intensity of light that will be sent into the zero diffraction order is given by $|A_0|^2 = \sin^2(M_A \pi)$ while the intensity of light sent into the first order is given by $|A_1|^2 = \sin^2[(M_A - 1)\pi]$. Figure 2(b) shows how the modulation depth of the grating affects both A_0 and A_1 . We further note that the modulation index M_A can vary

spatially [8] as shown in Fig. 2(c) and can allow amplitude information to be encoded onto both the zero and first order diffracted beams.

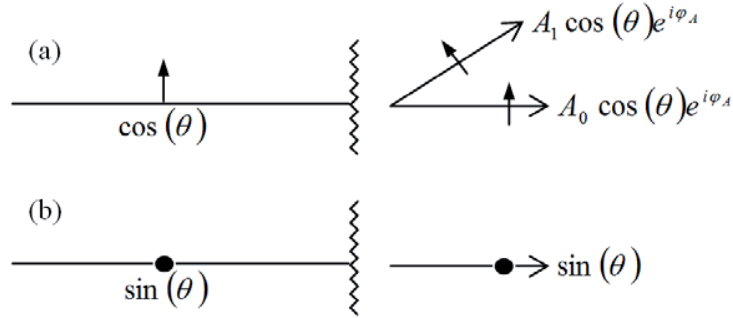


Fig. 1. Figure shows how (a) vertical and (b) horizontal polarization components of light are affected after passing through the LC-SLM that is encoded with a diffraction grating. Only the vertical polarization component is affected.

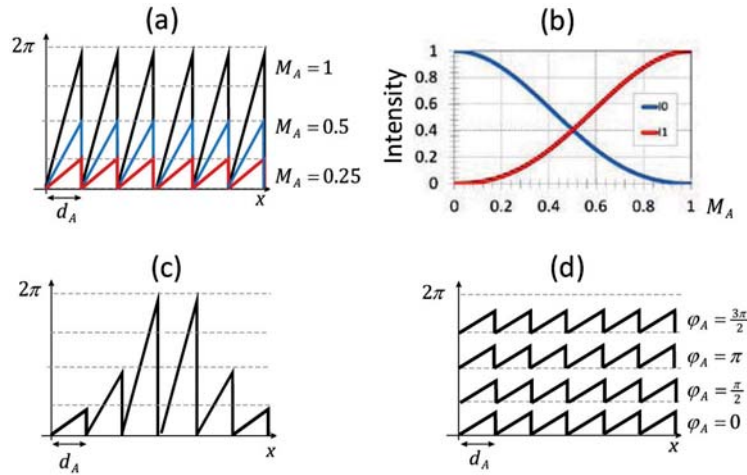


Fig. 2. (a) Blazed grating with variable depth of phase M_A and (b) corresponding intensity of the first and zero diffraction order versus M_A . (c) the diffracted light efficiency can vary spatially by applying a spatially variant blazed grating. (d) application of a phase bias φ_A to the blazed grating.

Secondly, we can add a phase bias φ_A to the grating as shown in Fig. 2(d). In this figure, we use the same modulation depth M_A for the phase grating. However the additional phase bias φ_A is then applied to both the zero and first diffracted orders, with no consequence in the transmitted intensity but with a major impact in the polarization state, as we show next. We again stress that the modulation index and the phase bias can both vary spatially.

As a result, we can write the Jones vector of the transmitted light in Eq. (1) as

$$E_A(x) = \begin{pmatrix} \cos(\theta) A_0 e^{i\varphi_A} \\ \sin(\theta) \end{pmatrix} + \begin{pmatrix} \cos(\theta) A_1 e^{i\varphi_A} \\ 0 \end{pmatrix} e^{i2\pi x/d_A}, \quad (1)$$

The left term shows the zero order diffracted beam while the right term shows the first order diffracted light. This expression shows that we have a subset of polarization control over the zero-order diffracted light for a fixed value of the incident angle θ of the polarizer. The LC-SLM can control the relative amplitude A_0 and phase φ_A of the vertical polarization component. We could obtain complete control over the polarization state of the zero-order diffracted light by inserting an electrically controlled polarization rotator into the system.

In our experiments, linearly polarized light from an Argon laser is spatially filtered, expanded, and collimated. The optical elements are encoded onto a parallel-aligned nematic LC-SLM manufactured by Seiko Epson with 640x480 pixels with pixel spacing of 42 microns [9]. Each pixel acts as an electrically controllable phase plate where the total phase shift exceeds 2π radians as a function of gray level at the Argon laser wavelength of 514.5 nm.

Figure 3 shows the general experimental setup. The collimated light passes through a linear polarizer and is incident onto the SLM that is encoded with a diffraction grating pattern. The first order diffracted light was removed using a spatial filter in the back focal plane of the first lens, and the transmitted light was imaged onto the detector. The output polarization state was examined using different polarizing elements in front of the CCD camera.

To demonstrate the potential of this approach, we created a two dimensional polarization map by dividing the screen of the SLM into 4 quadrants. Each quadrant of the SLM was programmed with a different phase bias added onto a blazed diffraction grating where $M_A = 0.5$ ($A_0 = 0.63$) [8]. We made the horizontal and vertical electric field components equal as $A_0 \cos(\theta) = \sin(\theta)$ by setting a polarization angle of $\theta = 32.5^\circ$. Now by varying the phase bias level from $\varphi_A = 0, \pi/2, \pi$ and $3\pi/2$, we can create various states of polarization ranging from linearly to circularly polarized light.

The mask is shown in Fig. 4(a). The gratings in the top right and bottom left quadrants have phase biases of $\varphi_A = 0$ and $\varphi_A = \pi$ and will generate linearly polarized light oriented at $+45^\circ$ and -45° respectively. The gratings in the top left and bottom right quadrants have phase biases of $\varphi_A = \pi/2$ and $\varphi_A = 3\pi/2$ and will generate right and left circularly polarized light respectively. This mask was encoded onto the SLM.

Figure 4(b) shows the output images taken through an analyzer polarizer oriented from $0^\circ, +45^\circ, 90^\circ, 135^\circ$, and then with right and left hand circular polarizer analyzers. Experimental results show that the 4 quadrants are producing the desired linearly and circularly polarized beams, as can be derived from the intensity transmission for each analyzer orientation. For instance, when the linear analyzer is set vertical or horizontal, a uniform intensity is obtained (although dark lines may appear on the quadrant edges whenever a phase discontinuity is created in the transmitted pattern [10,11]).

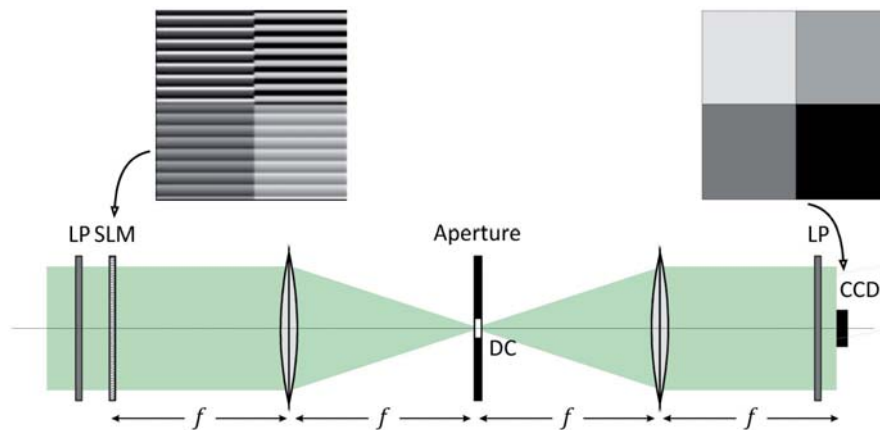


Fig. 3. Experimental configuration for the single pass experiment.

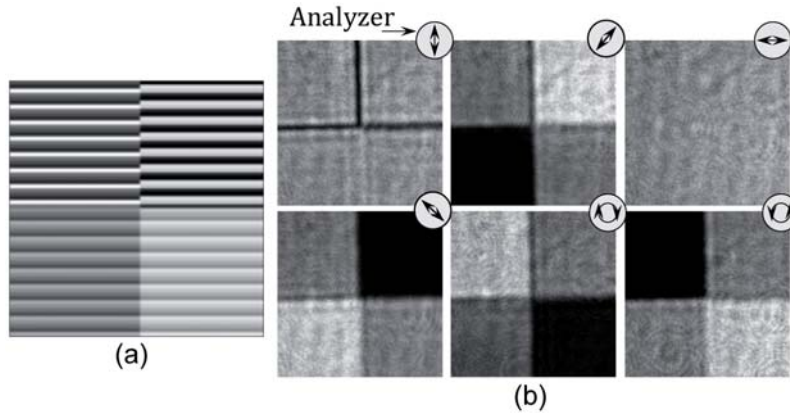


Fig. 4. (a) Grating mask. (b) Output images are shown using a linear polarizer analyzer oriented at 0°, 45°, 90°, 135° and with right and left circularly polarizer analyzers.

These experimental results show that we can create a two-dimensional polarization map with a single pass through the SLM. We emphasize that this system is completely programmable where each section of a two dimensional map can be programmed with different modulation indices and phase biases to create any desired array of elliptical polarization states. The number of regions can be increased, although there is an important limitation in that each area must contain a sufficiently large number of periods to achieve the ideal diffraction efficiency in order to obtain the desired effect in the zero order.

While this configuration allows excellent control of the zero order polarization state, we cannot control the polarization state of the diffracted light. The spatial control of the modulation depth of the grating only affects both A_0 and A_1 . The modulation depth of the grating only affects the vertically polarized light. In order to control the polarization states of the first order diffracted beams, we must utilize the double modulation scheme.

3. Double modulation theory and experimental results

Next, we show how further control may be gained for systems in which the light passes twice through the SLM (or through a second SLM). For that purpose, the transmitted beams from Fig. 1 are reflected and their polarization states are rotated by 90° by passing twice through a quarter wave plate. Now, the vertical polarization states become horizontally polarized, and the horizontal polarization state becomes vertically polarized. Note that an equivalent system in transmission would require two transmissive parallel aligned LC-SLMs, and a half-wave plate in between to switch polarizations.

In Fig. 5 we analyze the action of the same LC-SLM on the reflected light beams generated by the first passage through the SLM. Now, the retro-reflected light incident onto the SLM on this second passage shows reversed polarization components with respect to the light emerging from the SLM in the first pass (Eq. (1)). Therefore, the Jones vector describing the polarization of this retro-reflected incident light beam can now be written as

$$E = \begin{pmatrix} \sin(\theta) \\ A_0 \cos(\theta) e^{i\phi_A} \end{pmatrix} + \begin{pmatrix} 0 \\ A_1 \cos(\theta) e^{i\phi_A} e^{i2\pi x/d_A} \end{pmatrix}. \quad (2)$$

The initial vertical polarization component, which was previously diffracted by the first pass through the SLM, is now horizontally polarized and will pass through the SLM unaffected as shown in Fig. 5(a). Note that here we have two reflected beams with this polarization, corresponding to the zero and first orders generated in the first passage through the SLM. On the contrary, the horizontal component which was previously unaffected by the SLM will now pass through the SLM as vertically polarized light, and will diffract according

to the grating that is encoded onto this portion of the SLM. Note that there is only one reflected beam corresponding to this polarization.

If the reflected light is now incident onto a different area of the SLM screen, a second transmission function $t_B(x)$ can be encoded there in order to modulate the other polarization component of the light beam. This is a critical aspect of this configuration, as we are now allowed to program a different grating on this segment, and it can be programmed with its own modulation index M_B , that will affect the sizes B_0 and B_1 of the zero and first order diffracted beams as shown previously in Fig. 3. In addition, a different phase bias φ_B can be encoded onto this segment.

The orientation of this second diffraction grating can be changed as well, compared with the one that is encoded on the first segment of the SLM, so the light can be diffracted in a different direction. If the polarization states on these two first diffraction orders have different orientations, one pattern can be encoded with one polarization state while the other pattern can be encoded with another polarization state. That way it is possible to create polarization sensitive diffractive grating. On the contrary, if the orientations and periods of the gratings are equal, we can have the two first order diffracted beams overlap, allowing control of the composite polarization state of the output.

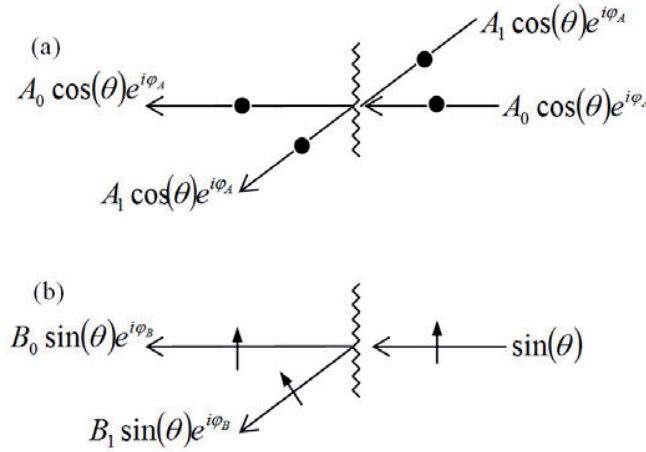


Fig. 5. Figure shows how (a) horizontal and (b) vertical polarization components of light are affected after passing a second time through a different part of the LC-SLM that is encoded with a different diffraction grating. The polarization states of Fig. 1 have been rotated by 90° . Again, only the vertical polarization component (which was the previous horizontal polarization component in the first pass) is affected.

For illustration purposes, we have chosen the same period and the same orientation for this second grating as $t_B(x) = \exp(iM_B 2\pi x/d_B)$, with $d_B = d_A = d_0$. Consequently, the light transmitted through the SLM on the second pass can now be written in Eq. (3) as:

$$E_B(x) = \begin{pmatrix} B_0 \sin(\theta) e^{i\varphi_B} \\ A_0 \cos(\theta) e^{i\varphi_A} \end{pmatrix} + \begin{pmatrix} \sin(\theta) e^{i\varphi_B} B_1 \\ \cos(\theta) e^{i\varphi_A} A_1 \end{pmatrix} e^{i2\pi x/d_0}, \quad (3)$$

where A_0 and A_1 represent the amplitude of the zero and first diffraction orders generated in the first pass, B_0 and B_1 represent the corresponding amplitudes generated in the second pass, and φ_A and φ_B represent the phase bias added in first and second pass respectively.

As before, the first term represents the Jones vector of the overall zero order diffracted light while the second term shows the Jones vector for the overall first order diffracted light. This result shows that we now have complete polarization control over both the zero and first-order diffracted beams. In addition, as mentioned earlier, we note that both modulation indices M_A and M_B , can vary spatially allowing amplitude information to be encoded onto

both polarization states, and both phase terms φ_A and φ_B can vary spatially and can be used to control the state of polarization in both beams. For simplicity, we choose $\theta = 45^\circ$.

The double modulation system, based on the previous polarization control discussion, will allow us to control the polarization of the first order diffraction and deepen control of the zero order beyond what was achievable with the single pass system. The key for this system is to divide the SLM into two parts. The experimental system is shown in Fig. 6.

Incident light passes through an aperture illuminating only the half of the SLM that is encoded with a transmission function $t_A(x)$, and will diffract the light as shown in Fig. 1. Note that half of the light is lost as it passes through a nonpolarizing beam splitter (NPBS). However this NPBS retains the polarization state of the incident light.

Both the diffracted and undiffracted orders pass through a lens and are reflected by a mirror placed in the focal plane of this lens. These rays pass twice through a quarter wave plate aligned to 45° that, upon reflection, behaves like a half wave plate. This effective half wave plate interchanges the horizontal and vertical linear polarization components. The returning rays are collimated by the lens and are now incident onto the other half of the SLM, which is encoded with the transmission function $t_B(x)$, diffracting the light as shown in Fig. 5. The transmitted light is now reflected towards the detector through the NPBS, again with its polarization states unchanged. The resulting light can either be imaged into a detector (similar to the single modulation experiment in Fig. 3) or the lens can form the Fourier transform of the patterns encoded onto the SLM (as shown in Fig. 6). We use this second approach in these experiments.

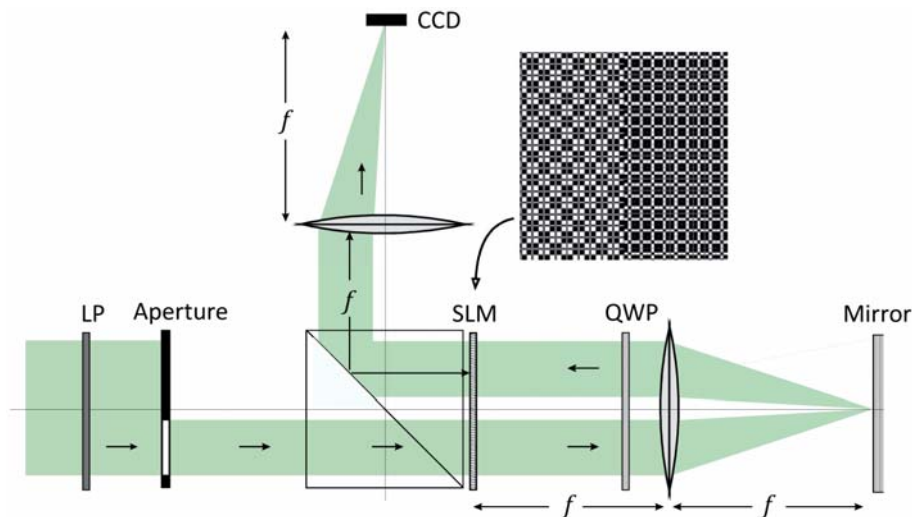


Fig. 6. Experimental configuration for the double pass experiment.

As stated earlier, the double modulation system gives us independent polarization control over both the zero order beam and the first order diffracted beam. We can individually vary the amplitude and phase of the vertical and horizontal components of the diffracted light by varying the parameters θ , M_A , M_B , φ_A , and φ_B . Also, note that the pattern diffracted through the first pass is now polarized horizontally, while the pattern diffracted through the second pass is polarized vertically.

Experimental results will be shown next.

3.1. Phase only polarization selective multiplexed computer generated holograms

We first show the capability of this system to act as a polarization selective computer generated hologram in order to form two images with different polarizations. We begin with two desired patterns written as $G_A(p, q - q_0)$ and $G_B(p, q + q_0)$ (here we use the letters

“SDSU” and “UMH” respectively) that are offset in opposite senses in the vertical direction, where q_0 is the offset parameter. We then take the Fourier transforms of the two images as $g_A(x, y) = \mathfrak{F}[G_A(p, q)] = |g_A(x, y)|e^{i\varphi_{gA}(x, y)}$ and $g_B(x, y) = \mathfrak{F}[G_B(p, q)] = |g_B(x, y)|e^{i\varphi_{gB}(x, y)}$. For this initial demonstration, we only encode the phase of each pattern ($\varphi_{gA}(x, y)$ and $\varphi_{gB}(x, y)$ respectively), each one on a different half of the SLM as shown in Fig. 7(a). Note that the gratings are implicitly encoded onto the Fourier transforms because of the initial offset of the images; in this case, since the offsets are in opposite sense, the corresponding linear phase gratings have opposite signs. If we were to take the Fourier transform of these phase-only holograms, we would obtain edge-enhanced images [12,13]. To avoid this edge-enhancement, we multiply the Fourier transforms by a random phase mask that successfully removes the edge enhancement effect [14].

In order to have equal intensity on both horizontal and vertical polarization components we selected the input polarization with an angle $\theta = 45^\circ$. In addition, since we are now encoding two phase-only patterns, we can apply the maximum modulation range and make $M_A = M_B = 1$, so the amplitudes in Eq. (3) become $A_0 = B_0 = 0$ and $A_1 = B_1 = 1$. Thus, the transmission of the system can be now rewritten as:

$$E_B(x, y) = \frac{1}{\sqrt{2}} \begin{pmatrix} e^{i\varphi_{gB}(x, y)} e^{-i2\pi x/d_0} \\ e^{i\varphi_{gA}(x, y)} e^{i2\pi x/d_0} \end{pmatrix} = e^{i\varphi_{gB}(x, y)} \frac{e^{-i2\pi x/d_0}}{\sqrt{2}} \begin{pmatrix} 1 \\ 0 \end{pmatrix} + e^{i\varphi_{gA}(x, y)} \frac{e^{+i2\pi x/d_0}}{\sqrt{2}} \begin{pmatrix} 0 \\ 1 \end{pmatrix}, \quad (4)$$

where d_0 is inversely related to the offset parameter p_0 . When the optical Fourier transform is produced by the last lens in Fig. 6, then the electric field can be written as

$$E_B(p, q) = \frac{1}{\sqrt{2}} (\delta(p - \gamma) \otimes G'_B(p, q)) \begin{pmatrix} 1 \\ 0 \end{pmatrix} + \frac{1}{\sqrt{2}} (\delta(p + \gamma) \otimes G'_A(p, q)) \begin{pmatrix} 0 \\ 1 \end{pmatrix}. \quad (5)$$

The $G'_A(p, q)$ and $G'_B(p, q)$ terms represent the images recovered from the Fourier transforms of the phase terms $e^{i\varphi_{gA}(x, y)}$ and $e^{i\varphi_{gB}(x, y)}$ multiplied by the random phase patterns respectively. The convolution simply shifts the center of the image to the location of the delta function. Equation (5) shows that all of the light diffracted by the grating on the right half of the SLM is located in the +1 vertically diffracted order and is horizontally polarized, while all of the light diffracted by the grating on the left half of the SLM is located in the vertically diffracted -1 order and is vertically polarized.

Figure 7(a) shows the phase-only mask, where the two halves correspond to the two generated phase-only holograms. Experimental results for this case are presented in Figs. 7(b), 7(c) and 7(d) when an analyzer polarizer is placed before the CCD camera that is oriented horizontally, at an angle of 45° , and vertically. These results show that the diffracted image of “SDSU” is horizontally polarized, while the diffracted image of “UMH” is vertically polarized.

Figure 7(e) shows another example of this polarization selective diffraction. Here we encoded two different Dammann gratings [15,16] on each side of the SLM. In one side the grating is designed to produce a 5x5 pattern of equally intense diffraction orders. In the other side a Dammann grating is designed to produce a 4x4 pattern. These are binary phase gratings with a π phase shift. The experimental results in Figs. 7(f), 7(g) and 7(h) show that the corresponding patterns of diffraction orders are being generated. However the 5x5 pattern is linearly polarized in the horizontal direction (Fig. 7(f)), while the 4x4 pattern is linearly polarized in the vertical direction (Fig. 7(h)). When the analyzer is oriented at 45° , all 41 diffraction orders are present (Fig. 7(g)).

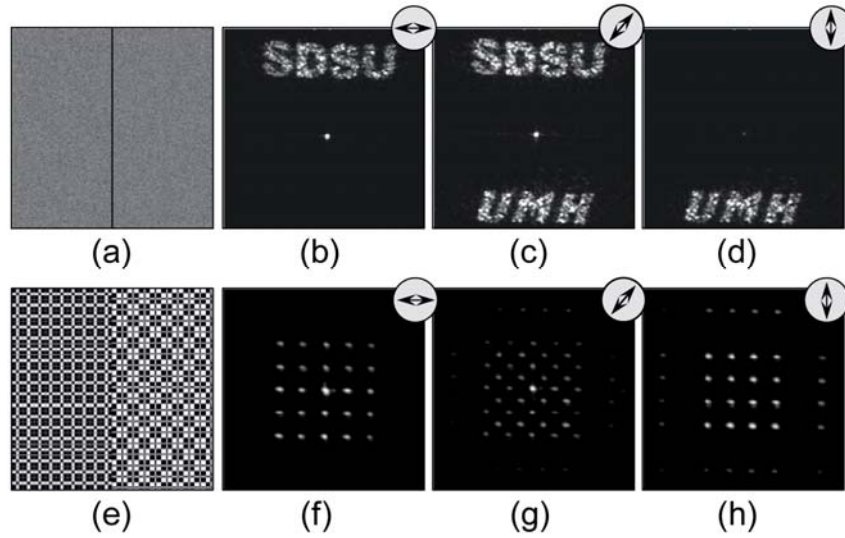


Fig. 7. Mask and experimental results from the double modulation polarization control when encoding two polarization sensitive diffractive elements. (a)-(d) the Fourier transform computer generated holograms reproducing letters “SDSU” and “UMH”; (e)-(h) 2D Dammann gratings with 4x4 and 5x5 diffraction orders. The analyzer polarizer is oriented horizontally in (b) and (f), at 45° from the vertical axis in (c) and (g) and vertically in (d) and (h).

3.2. Computer generated holograms reconstruction with polarization control

Now we can show the full capability of this system to generate an output image having an arbitrary polarization state as suggested from Eq. (3). As before, we use the letters “SDSU” and only encode the phase of these holograms. We again multiply the letters by a random phase pattern to remove the edge enhancement. Here, we encode the Fourier transform of the same pattern onto both halves of the SLM. However now we provide different phase biases to the patterns. We begin with the same conditions as before ($\theta = 45^\circ$ and $M_A = M_B = 1$, so $A_0 = B_0 = 0$ and $A_1 = B_1 = 1$) but now we select the same pattern to be encoded on both sides of the SLM, and insure that their Fourier transforms will overlap, i.e., $\varphi_{g_A}(x, y) = \varphi_{g_B}(x, y) = \varphi_g(x, y)$ and $d_A = d_B = d_0$. However we can also add an additional uniform phase relative between the two halves of the screen (either by φ_A or φ_B). Then, Eq. (4) changes to:

$$E_B(x, y) = \frac{1}{\sqrt{2}} \begin{pmatrix} e^{i\phi_g(x, y)} e^{i\phi_B} e^{+i2\pi x/d_0} \\ e^{i\phi_g(x, y)} e^{+i2\pi x/d_0} \end{pmatrix} = e^{i\phi_g(x, y)} \frac{e^{+i2\pi x/d_0}}{\sqrt{2}} \begin{pmatrix} e^{i\phi_B} \\ 1 \end{pmatrix}, \quad (6)$$

where we selected φ_B to control the output polarization. As a result, the electric field at the Fourier transform plane is given by:

$$E_B(p, q) = [\delta(p - \gamma) \otimes G'(p, q)] \frac{1}{\sqrt{2}} \begin{pmatrix} e^{i\phi_B} \\ 1 \end{pmatrix}. \quad (7)$$

This equation shows that a single pattern is being produced, at the location $p = \gamma$, but the state of polarization is dependent on the phase bias φ_B .

Figure 8 shows the experimental results when the phase masks on both sides of the SLM are designed to produce the same “SDSU” pattern at the same location. However we show four cases (the four rows of the figure) where we added phase bias values $\varphi_B = 0, -\pi/2, -\pi,$ and $-3\pi/2$. According to Eq. (7), these phase bias values produce the diffraction pattern with 4

polarization states corresponding to linear polarization at 45° , right circularly polarized, linear polarization at 135° , and left circular polarized respectively. Each column in Fig. 8 corresponds to the image captured with the CCD when an analyzer is placed just in front of it. A linear polarizer oriented at 0° , 45° , 90° and 135° , and two R and L circular polarizer analyzers have been employed. These results probe that the SDSU pattern is being generated with the state of polarization defined by the phase bias φ_B . Experimental results confirm that each image in the different rows is polarized as expected.

It must be noted, however, that to achieve these results it has been necessary to very accurately align the system. Otherwise, interference fringes appear over the reconstructed pattern.

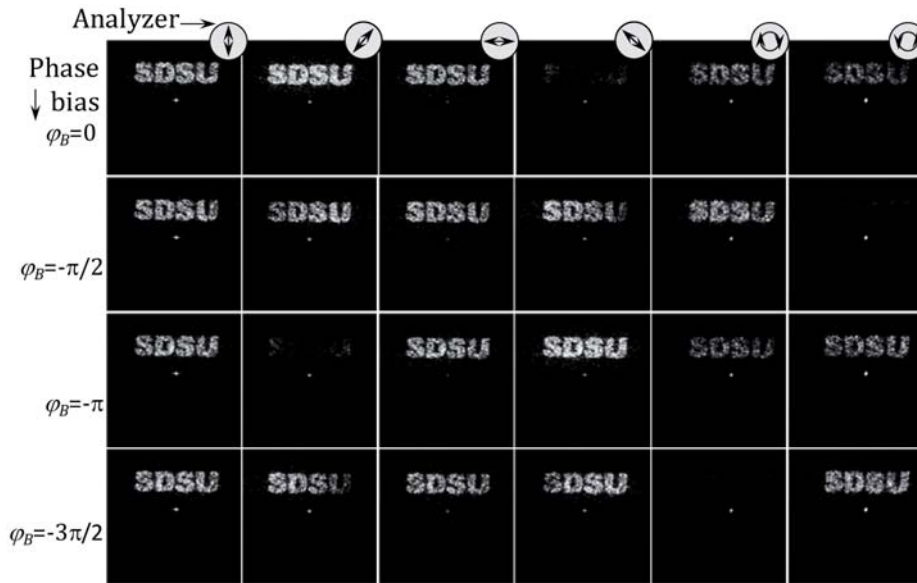


Fig. 8. Experimental results when the same pattern “SDSU” is encoded on both sides of the SLM, but a phase bias φ_B is added on one side with respect to the other (corresponding to the different rows). In each column an analyzer polarizer is placed before the CCD, linear at 0° , 45° , 90° and 135° , and circular right and left.

3.3. Fully complex polarization computer generated holograms

As a final example of the potential uses of the proposed setup we include here a case where both amplitude and phase information is encoded onto each of the polarization components. For that purpose we follow the technique in Ref [8], and previously employed in Section 2, to encode the amplitude information onto the corresponding phase component.

Figure 9 present equivalent results to those in Fig. 8. But now the object to be reproduced is a rectangle. In order to generate this rectangle, a sinc() type amplitude function must be encoded in the phase grating. But in order to obtain a control on the polarization state of the generated rectangle, this must be encoded on both polarization components. For this purpose we generate a phase mask like that shown in Fig. 9(a). First the sinc() function is centered on each half of the SLM screen so the light beam on each passage gets fully diffracted to reproduce the rectangular shape. Then amplitude parameters $M_A = M_B$ are selected to match the sinc function and the nonlinear M to M' function is applied to perfectly match the complex function on the first diffraction order [8].

Figure 9(b) shows the experimental results obtained with this phase mask. The rectangle is located in the lower right quadrant of each image. We also see the large DC component that is generated by the zero order when using the approach in Ref [8]. Again, a precise alignment of the system is required to avoid interference fringes at the rectangle reconstruction. Additional

phase bias values $\varphi_B = 0, -\pi/2, -\pi,$ and $-3\pi/2$ have also been added in one half of the phase mask. Therefore, according to Eqs. (6)-(7), the output rectangle will have 4 polarization states corresponding to linear polarization at 45° , right circularly polarized, linear polarization at 135° , and left circular polarized respectively. Different columns in Fig. 9(b) correspond to the experimental result when a different analyzer is placed before the CCD. From left to right, the results correspond to linear polarizer analyzers oriented at $0^\circ, 45^\circ, 90^\circ$ and 135° , and circular R and L polarizer analyzers.

These experimental results show that the rectangular shape is being generated in all cases, and its state of polarization is fixed by the phase bias φ_B , being linearly polarized at $\pm 45^\circ$ when $\varphi_B = 0$, and $-\pi$, and circularly polarized (R and L) when $\varphi_B = -\pi/2$, and $-3\pi/2$.

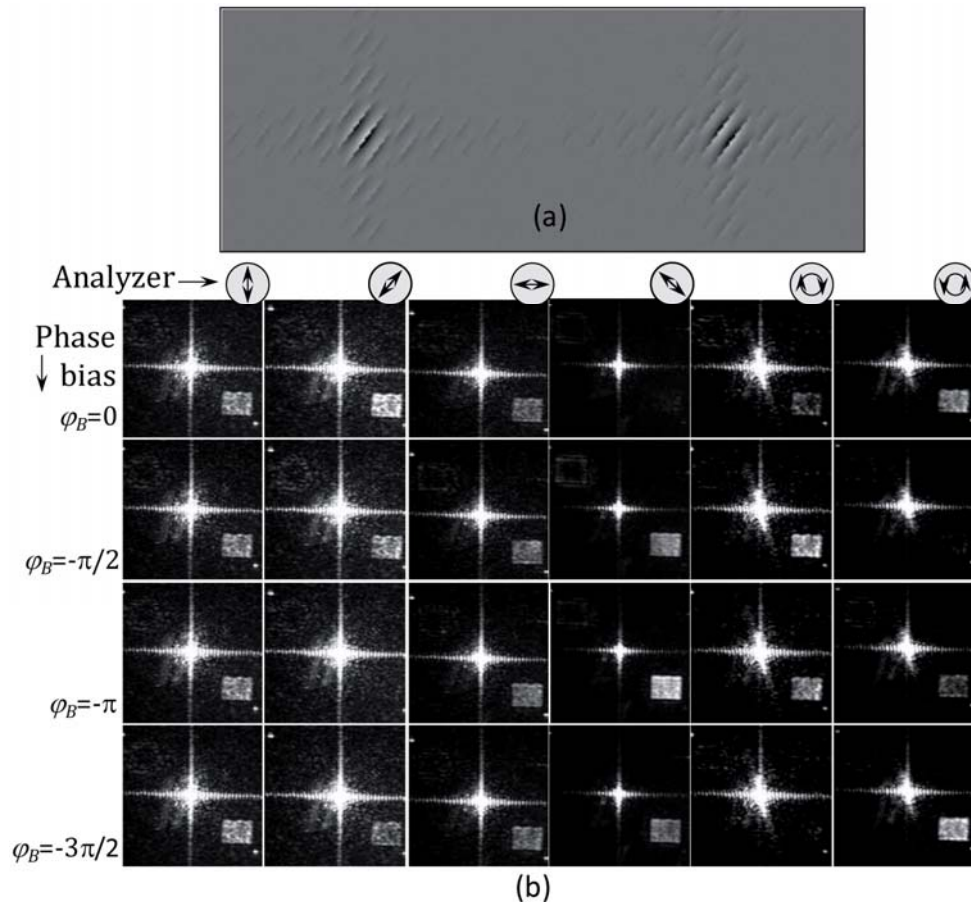


Fig. 9. (a) Central detail of the phase mask displayed on the SLM. (b) Experimental results when the same amplitude and phase pattern designed to generate a rectangle is encoded on both sides of the SLM, but with a phase bias φ_B added on one side relative to the other. In each column an analyzer polarizer is placed before the CCD, linear at $0^\circ, 45^\circ, 90^\circ$ and 135° , and circular right and left.

4. Conclusions

In summary, we have shown the possibility to achieve total spatial polarization control with a diffractive optical system based on a single parallel aligned liquid crystal display. We first studied the control that can be achieved with a single pass through the device, where one polarization component can be fully controlled via a linear phase grating with encoded amplitude. Then, the study is extended to a double modulation scheme, where a quarter-wave

plate is added to interchange orthogonal linear polarization components upon reflection. In this way, the two polarization components can be fully modulated and a full control over the polarization state is obtained. Several experiments showing various characteristics of polarization sensitive computer generated holograms have been proposed that demonstrate the characteristics of the proposed setup. The full polarization control achieved by this system opens the possibility to produce programmable polarization sensitive holographic patterns.

We expect that this double modulation approach can be extended to produce multiple objects in the output plane, each with a controllable polarization state. This approach seems limited only by the number of pixels in the SLM.

The success of this approach lies in the fact that only one polarization state is affected during each pass through the SLM. The other polarization state is unaffected. After passing through the double quarter-wave plate, the unaffected polarization state is now acted upon by the SLM while the other state remains encoded.

There are alternative configurations that might be used. One might more conveniently use two transmissive parallel aligned LC-SLMs with a half-wave plate simply placed between them. However we are not aware of any manufacturers of transmissive parallel aligned LC-SLMs. Ours is a prototype model produced by Seiko-Epson. The parallel aligned LC-SLM has the advantage that the orthogonal polarization state is unaffected by the SLM.

One might use the more common transmissive twisted-nematic LC-SLMs. However in order to achieve phase-only operation, we require appropriately aligned linear polarizers and quarter-wave plates on either side of the TNLCD in order to create and detect the polarization eigenvector with the largest phase shift variation [17]. The orthogonal polarization eigenvector has some weak polarization and phase dependence [18,19]. Therefore at best, one would have to compensate for this unintended polarization encoding.

An alternative configuration would require two reflective parallel-aligned LC-SLMs. These are available from a small number of manufacturers, but are quite expensive.

If the results of this study prove extremely valuable, then they might encourage either manufacturers to rethink the utility of transmissive parallel aligned LC-SLMs or an increase in the popularity of reflective devices with a corresponding price reduction.

In any event, these results should increase interest in the polarization control that can be achieved with programmable devices.

Acknowledgments

We thank Tomio Sonehara of Seiko Epson Corporation for the use of the LC-SLM. Ignacio Moreno acknowledges financial support from Spanish Ministerio de Ciencia e Innovación (grant FIS2009-13955-C02-02).